EACWE 5
Florence, Italy
19th – 23rd July 2009

Reynolds number dependence of the velocity shear effects on flow around a circular cylinder

[1] Shuyang CAO, [2] Yukio TAMURA
[1] *Shuyang@tongji.edu.cn, State Key Lab for Disaster Reduction in Civil Engineering, Tongji University, China*
2 Wind Engineering Research Center, Tokyo Polytechnic University, Japan

Keywords: Aerodynamic force, Direct Numerical Simulation, Large Eddy Simulation, Shear parameter, Wake dynamics.

ABSTRACT

Three-dimensional Direct Numerical Simulation (DNS) and Large Eddy Simulation (LES) are performed to investigate the shear effects on flow around a circular cylinder at Reynolds numbers of Re=60-1000. The shear parameter β, which is based on the velocity gradient, cylinder diameter and upstream mean velocity at the center plane of the cylinder, varies from 0 to 0.30. Variations of Strouhal number, drag and lift coefficients, and unsteady wake structures with shear parameter, and their dependences on Reynolds number, are studied. Present simulation not only confirms our previous experimental findings, but also provides new and detailed information of the flow around a cylinder circular in shear flow with respect to the effects of both velocity shear and Reynolds number. It is shown that the Strouhal number has no significant variation with shear parameter. The stagnation point moves to the high-velocity side almost linearly with shear parameter and this mainly influences the aerodynamic forces acting on a circular cylinder in shear flow. Reynolds number has little influence in determining the movement of the stagnation point but plays important roles in the movement of the separation point. Mode A wake instability at Re=200 was suppressed into a parallel vortex shedding mode in strong shear flow.

Contact person: Shuyang Cao, State Key Lab for Disaster Reduction in Civil Engineering, Tongji University, China 1239 Siping Road, Shanghai 200092, China. TEL: +86 21 65983116 Ext.2317, FAX: +86 21 65984882 numbers. E-mail Shuyang@tongji.edu.cn

1. INTRODUCTION

Vortex shedding behind two-dimensional circular cylinders has been one of the most studied subjects in fluid mechanics in the past several decades because of its practical and theoretical importance. Although quite comprehensive understanding of the vortex dynamics in a cylinder's wake have been achieved, as reflected in the reviews by Williamson (1996) and many other researchers, the simplicity of the geometry and the abundance of interesting flow features continue to make this flow the subject of many current studies. The majority of past studies on unsteady flow past a circular cylinder were conducted under symmetric approaching flow conditions in which vortices are equivalently shed from each side of the body. However, in many practical applications, a cylindrical structural is immersed in a flow with some asymmetries. For example, a bridge deck is located in an atmospheric boundary layer with a velocity shear profile. Since strong local shear flows can be produced by special metrological phenomena, terrain effect and so on, it is important to understand the features of vortex shedding behavior and aerodynamic forces on a circular cylinder in a shear flow. Meanwhile, how the velocity shear, a simple and typical case of a non-uniform approach flow, influences vortex shedding from a circular cylinder and wake dynamics is also a very interesting fundamental problem. With increase in velocity shear, the velocity difference between the high- and low-velocity sides of a cylinder increases. The strength and depth of the boundary layer on the two sides, and then the vorticity generated in the separated shear layers, differ on the two sides. This possibly creates differences in vortex shedding behavior or shear layer instability on the two sides of a cylinder. This study was motivated by the need to understand these behaviors both theoretically and practically. In this paper, the extent of velocity shear is expressed by the shear parameter $\beta = G(D/U_c) = (dU/dy)(D/U_c)$, where U_c is the mean velocity at the center plane, D is the diameter of the circular cylinder and G is the velocity gradient, as illustrated in Fig.1. The origin of the coordinate system is the center of the circular cylinder.

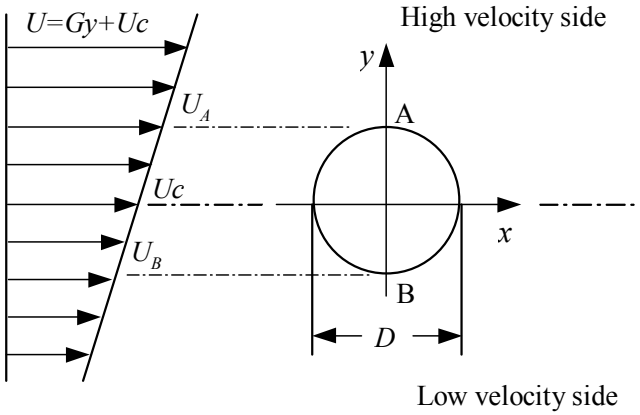

Fig.1. Schematic of shear flow configuration

Several experimental studies have been carried out on the shear effects on flow around a circular cylinder. However, there has been significant disagreement among the results, even on basic issues associated with vortex shedding behavior. Kiya et al. (1980) investigated vortex shedding from a circular cylinder in moderate Reynolds number shear flows (Re=35-1500) in a water tank. They found that the critical Reynolds number for vortex shedding to take place is higher in shear flow than in uniform flow. They also found that the Strouhal number decreases slightly with shear parameter when the shear parameter is small, and then clearly increases with shear parameter at large shear parameter. Kwon et al. (1992) reported similar results for $0.05 < \beta < 0.25$ at Re = 35-1600. Adachi and Kato (1975) investigated the flow around a circular cylinder within a small variation in shear parameter ($0 < \beta < 0.04$) at Re= 2.67×10^3-1.07×10^4. They reported that both mean drag and lift force increase with shear parameter, and lift force acts from the high-velocity side to the low-velocity side.

Hayashi and Yoshino (1990) investigated the aerodynamic force in one kind of shear flow (β =0.15) at Re=6×10^4 and found that drag decreases in shear flow and lift force acts from the high-velocity side to the low-velocity side. The study of Sumner and Akosile (2003) at Re=4.0×10^4-9.0×10^4 with a low shear parameter range of β =0.02-0.07 showed conclusions with regard to drag and lift forces similar to those of Hayashi and Yoshino (1990), but Strouhal number is shown to be almost unchanged with shear parameter. There have been fewer numerical studies and they have been restricted to two-dimensional calculations. However, their results have also been inconsistent. Tamura et al. (1980) performed a numerical study on shear flow past a circular cylinder at Re=40 and 80 for $0<\beta<0.20$. Lei et al. (2000) carried out two-dimensional simulation of flow at Re=80-1000 for $0<\beta<0.25$ with an upwind scheme. Both studies indicated that the front stagnation point moved to the high-velocity side in the shear flow. However, they reported different results in regard to the direction of lift force. Lei et al. (2000) found that the lift was toward the low-velocity side, while Tamura et al. (1980) reported that it was in the opposite direction. The disagreements in both experimental and numerical studies also motivated the present study.

Our experimental study (Cao et al., 2007) at Re=3.4×10^4 within a wider shear range ($0<\beta<0.27$) showed that the flow and aerodynamic force around a circular cylinder was subject to the combined effects of the movement of stagnation point and velocity shear, which acts in the opposite direction to the aerodynamic force. Thus, many factors, including Reynolds number, body shape and geometry, which may influence the individual contributions of the movement of stagnation point and velocity shear to pressure distribution, influence the effects of velocity shear in the oncoming flow, resulting in different conclusions. We infer that this as a possible reason for the inconsistencies of past studies. However, there are still many unknowns and further detailed study is necessary on this flow configuration.

In this study, we systematically performed three-dimensional Direct Numerical Simulation (DNS) and Large Eddy Simulation (LES) calculations to investigate the effects of velocity shear on vortex shedding from a circular cylinder and wake dynamics. From detailed flow information obtained by numerical simulation, we expect to achieve a comprehensive understanding and arrive at a physical explanation of the mechanism of shear effects. In the numerical simulation, a co-locate mesh was employed in the generalized coordinate system for finite difference approximation of the incompressible Navier-Stokes equations. The simulation was carried out for Re=60, 80, 150, 200, 500 and 1000 to investigate the Reynolds number dependence, which was one possible reason for the inconsistencies in past studies. DNS was performed for Re=60, 80, 150 and 200, while LES was carried out with a dynamic Smagorinsky subgrid model for Re=500 and 1000. A central difference scheme was applied in the simulation in order to avoid unnecessary numerical dissipation accompanying the upwind scheme. More accurate yet stable simulation can be expected from the central difference scheme as shown by Kravchenko and Moin (2000) in their numerical studies of flow over a circular cylinder at Re=3900. However, the Reynolds number has generally been limited to 103 for the central difference scheme till now. Therefore, the Reynolds numbers considered in the present study are up to Re=1000 in order to achieve more precise and stable predictions of shear effects. The governing equations in the generalized coordinate system and corresponding numerical procedure are described first, followed by detailed validations. Then, the shear effects on Strouhal number, aerodynamic force, and the corresponding physical mechanism are presented, together with illustrations of the dynamic wake structure.

2. FORMATION AND NUMERICAL DETAILS

The numerical model for flow around a circular cylinder is formulated using the generalized curvilinear coordinate system. The governing equations are the continuity and Navier-Stokes equations. We utilized the non-staggered-grid method developed by Zang et al. (1994) for solving three-dimensional, time-dependent incompressible Navier-Stokes equations for unsteady calculations in curvilinear coordinates. In the computational space, the Cartesian velocity

components and the pressure are defined at the center of a control volume, while the volume fluxes are defined at the mid-point of their corresponding cell surface. Fourth-order central difference and fourth-order interpolation are used for the convection terms while a second-order central differencing scheme is used for the diffusion terms. The continuity equation is discretized at the point where pressure is defined using contravariant velocity components. For time marching, the explicit Adams-Bashforth differencing scheme is applied for the convention term, and the semi-explicit Crank-Nicolson formulation is applied for the diffusion term.

The dynamic procedure based on the Smagorinsky model proposed by Germano et al. (1991) is used. The ratio of test filter scale to grid filter scale is the only parameter in the procedure and is chosen to be 2.0, as suggested by Germano et al. (1991). Averaging and test filter operation are performed only in the homogeneous spanwise direction, in conjunction with Lilly's least-squares technique (1992). In order to avoid numerical instability, the negative value of SGS eddy viscosity is truncated to zero. Large Eddy Simulation using the dynamic Smagorinsky model has been widely utilized as a relatively affordable and easy-to-use approach to simulate separated flow and other complicated flow (Kravchenko and Moin 2000)

To adequately resolve the flow, an O-type body-fitted grid system is used. The computational domain is basically 30*D* on the circular plane by 4*D* in the spanwise direction for all Reynolds numbers, but the spanwise domain is 8*D* for Re=200. The vortex instability experiences mode change in the Reynolds number range of 50<Re<1000, and one feature of mode A instability at Re=200 is the 4*D* wavelength structure in the wake in the spanwise direction. Therefore, the computational domain in the spanwise direction is set to 8*D* for Re=200 in order to illustrate mode A wake dynamics more directly. Grid number on the circular plane is 160×140 for all Reynolds numbers, while it is 40 or 80 in the spanwise direction, depending on whether the computational domain is 4*D* or 8*D*. The size of the first grid near the body surface is $0.1/\sqrt{\mathrm{Re}}$, and it stretches outwards to the boundary.

The boundary conditions for simulation are as follows:

Cylinder body surface: No slip condition for velocity; Neumann condition for pressure;

Inlet: Specified mean velocity profile; Neumann condition for pressure;

Outflow boundary: Convective boundary condition of the form $\frac{\partial}{\partial t}+c\frac{\partial}{\partial x}=0$ is applied for velocity and pressure. In order to ensure global mass conservation, *c* is taken to be the bulk velocity.

Spanwise: Periodic condition for velocity and pressure;

In addition, proper boundary conditions for the intermediate (split) velocity field, $u_i^* = u_i^{n+1} + \Delta t\,\partial\phi^n/\partial x_i$ proposed by Kim and Moin (1985) to guarantee the precision of discretization, are imposed.

Detailed algorithm and validation can be found in the papers of Cao and Tamura (2008, 2009).

3. NUMERICAL RESULTS AND DISCUSSIONS

3.1 Vortex shedding in shear flow

Fig.2a shows the variation of Strouhal number, S_t, with shear parameter at Re=60, 150, 200, 500 and 1000. Strouhal number is defined as $S_t = f \times D/U_c$, where vortex shedding frequency *f* is detected from the aerodynamic force on the cylinder by FFT. Fig.2 shows that the Strouhal number has a very small decrease or increase with shear parameter at all Reynolds numbers although its magnitude varies due to Reynolds number dependence. Meanwhile, discontinuity in the change of Strouhal number with shear parameter can be observed at Re=200. The variation of Strouhal number is so small that the Strouhal number can be considered unchanged with shear parameter at these Reynolds numbers. The observations of Strouhal number of past studies are shown in Fig.2b for comparison. The results of the present study agree with those of the experimental studies of Sumner and Akosile (2003) and ourselves (Cao et al., 2007) at higher Reynolds number, and show little difference from the numerical results of Lei et al. (2000) in the same Reynolds number regime. Lei et

al. (2000) conducted 2*D* simulation and showed that the Strouhal number decreased with shear parameter, but very slightly: in the order of a few percent. However, the present results clearly contradict the results of Kiya et al. (1980). In their experimental study, Kiya et al. (1980) found that vortex shedding disappeared for sufficiently large shear parameters, for instance, the case of β=0.15 at Re=79, and the critical Reynolds number, above which vortex shedding occurs, depends on shear parameter. Meanwhile, they observed obvious variation of Strouhal number, as shown in Fig.2b. The present results show that vortex shedding never disappears, even under very large shear parameter, at low Reynolds number. Actually the phenomenon of Karman vortex shedding being completely suppressed in shear flow never occurred in numerical simulations, including the 2D simulation of Lei et al. (2000) and the numerical work of Kiya's group themselves (1980). It seemed to the authors that there was some kind of mismatch between the numerical studies and the experimental studies on the shear flow over a circular cylinder.

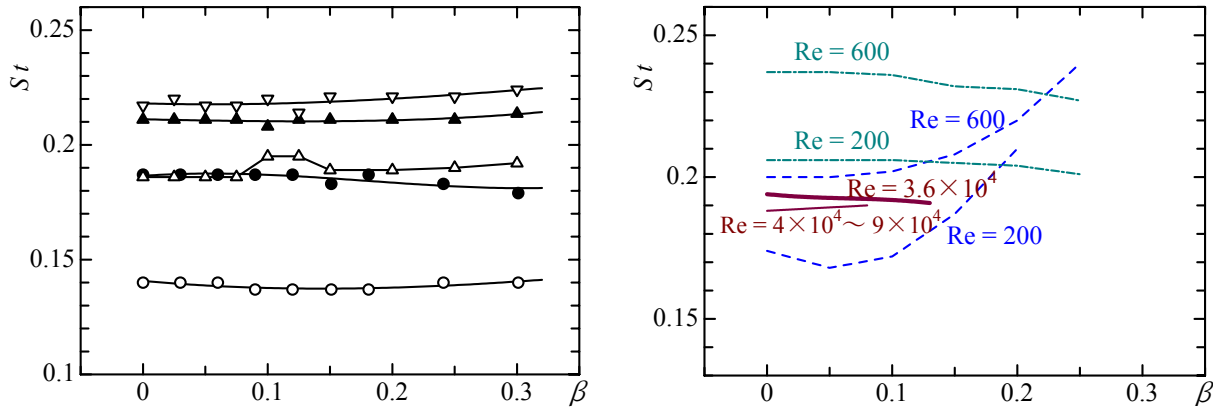

(a) Results of present simulation (○: Re=60; ●: Re=150; △: Re=200; ▲: Re=500; ▽: Re=1000)

(b) Results of past studies (---- : Kiya et al., 1980; -·-·- :Lei at al., 2000; ▬ : Cao et. al., 2007; —— : Sumner and Akosile, 2003)

Fig.2 Variation of Strouhal number with shear parameter

However, we observe some evidence of suppression of three-dimensionality by velocity shear from the results at Re=200, a transient Reynolds number, which is related to the discontinuity of the change of Strouhal number at Re=200, as plotted in Fig.2a. Fig.3 compares the iso-vorticity surface of the instantaneous near-wake structure at β=0 (Non-shear flow), β=0.05, β=0.1 and β=0.2 at Re=200. The wavelength is about 4.0*D* under the non-shear flow condition, as shown in Fig.3a. With increase in shear parameter, for instance at β=0.05, the braid between Karman vortices becomes simpler in structure. The variation of three-dimensionality in the spanwise direction of both the Karman vortices and streamwise vortices becomes very unitary, i.e. only the 4*D* wavelength pattern in the spanwise structure can be observed, with almost all other wavelength components being suppressed (Fig.3b). The wake structure changes to the 2-dimensional parallel vortex shedding mode at β=0.1 (Fig.3c). This means that the onset of mode A was suppressed by the shear parameter. Present study is, to the author's knowledge, the first one that reports the suppression of three dimensionality of the wake of a circular cylinder in shear flow. With further increase in shear parameter, for instance at β=0.2, the variation of Karman vortex in the spanwise direction is suppressed (Fig.3d), in a similar manner to that at β=0.1, but a kind of regular variation of streamwise vortex structure in the spanwise direction is observed. However, its relation to shear parameter or vortex shedding behavior is unknown. Compared to Re=200, due to the original complication of the spanwise structure at high Reynolds number, we could not observe a distinct phenomenon of suppression of three dimensionality at Re=1000.

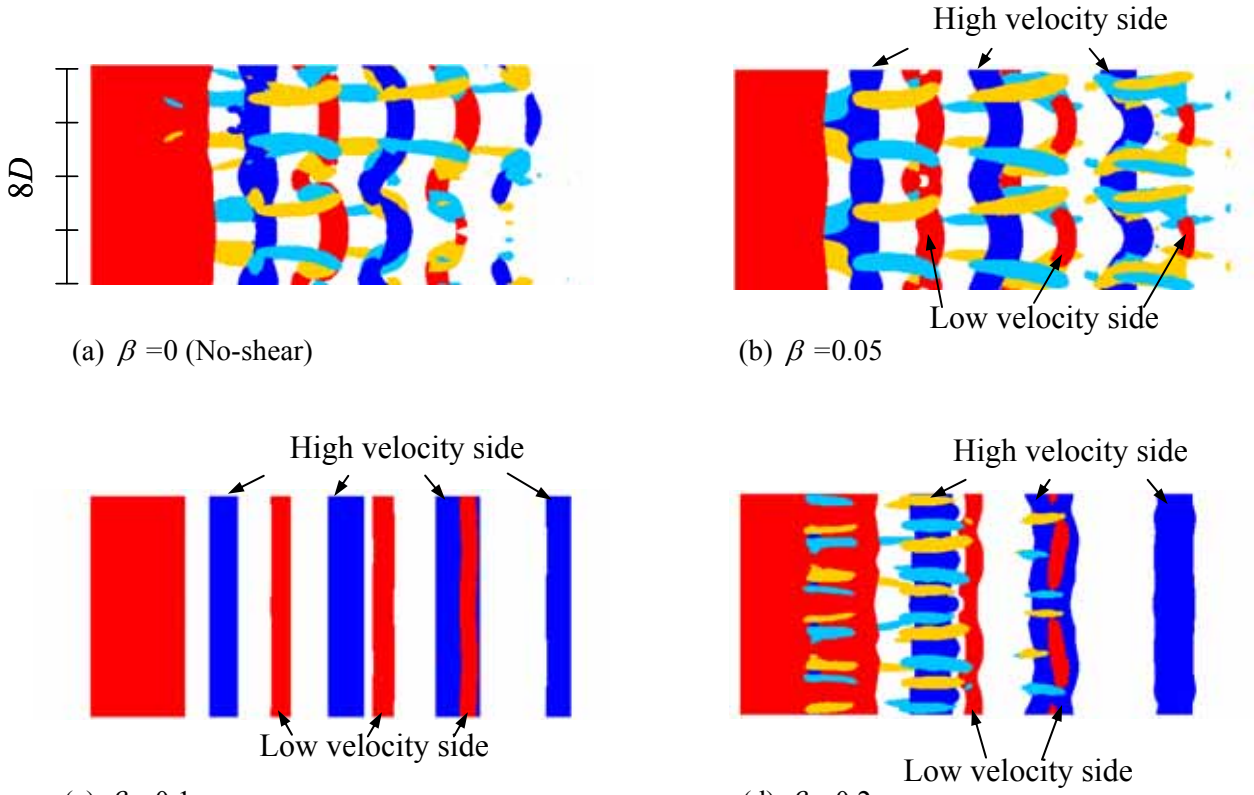

(a) β =0 (No-shear) (b) β =0.05

(c) β =0.1 (d) β =0.2

Fig.3 Variation of iso-vorticity surface of instantaneous wake structure with shear parameter at Re=200

On the other hand, it is observed in Fig.3 that the distance between Karmax vortices on the high-velocity side is different from that on the low-velocity side, due to the different advection velocities on the two sides. This causes instability in the Karman vortex street and results in complicated turbulence structures in the far wake, which is important when considering the environmental disturbance downstream of a large structure. It can also be observed that the vortices on the low-velocity side become very weak and small compared to their counterparts on the high-velocity side, at the relatively far wake of the cylinder. The vortices on the low-velocity side even disappear under the strong shear condition. This phenomenon can be explained as a result of interaction of separated vortices with opposite rotation direction on the two sides of the cylinder with the vortices in the oncoming shear flow (Cao et al., 2007). However, the present study shows that, in the near wake of the cylinder, the Karman vortex shedding behavior is never completely suppressed at $0<\beta<0.3$ at Re=60-1000.

As observed in our previous experimental work (Cao et al. 2007), the movements of the stagnation point and separation points are significant phenomena for flow around a circular cylinder under the influence of velocity shear in the oncoming flow. The movement of stagnation point with shear parameter at all investigated Reynolds numbers is shown in Fig.4, where θ_0 is the flow stagnation point angle. The flow stagnation point is not at the geometrical stagnation point in the shear flows. Fig.4 shows that the stagnation points moves to the high-velocity side in shear flow, and the stagnation point angle increases almost linearly with shear parameter for all Reynolds numbers. At low Reynolds numbers, the stagnation point angle decreases with increasing Reynolds number for a given shear parameter, but becomes almost constant when the Reynolds number is larger than Re=500. This means that the movement of the stagnation point is mainly determined by the shear parameter. Reynolds number effect on the movement of stagnation point is small.

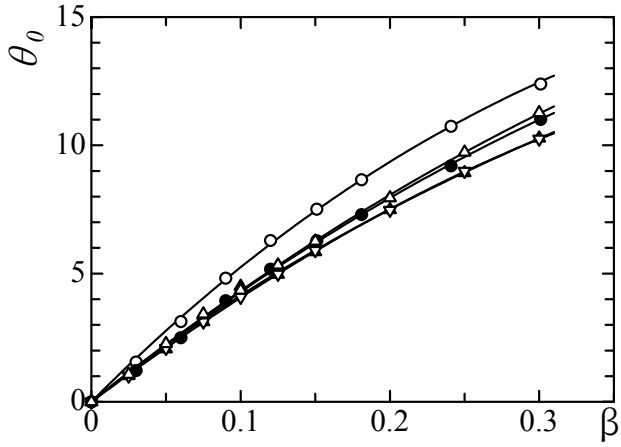

Fig.4 Movement of stagnation point with shear parameter
(○: Re=60; ●: Re=150; △: Re=200; ▲: Re=500; ▽: Re=1000)

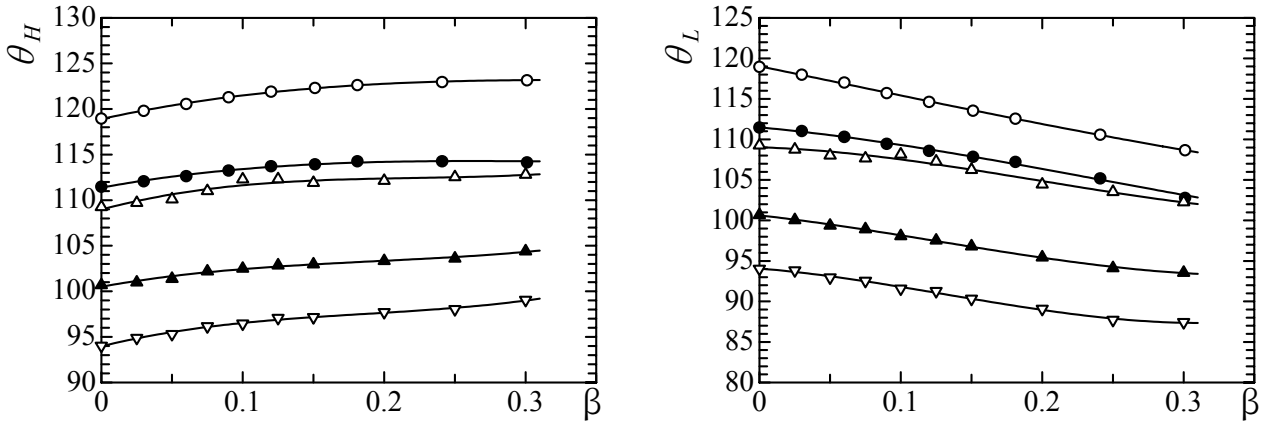

(a) High velocity side (b) Low velocity side

Fig.5 Variation of separation point with shear parameter
(○: Re=60; ●: Re=150; △: Re=200; ▲: Re=500; ▽: Re=1000)

Fig.5a and Fig.5b show the variation of separation points with shear parameter on the high- and low-velocity sides individually. θ_H and θ_L are the angles of the separation points on the two sides. The separation point moves downstream on the high-velocity side and upstream on the low-velocity side, almost linearly with shear parameter. As in the non-shear condition, the separation points on both the high- and low-velocity sides move upstream, almost linearly with the logarithm of Reynolds number at Re=60-1000. The Reynolds number greatly influences the movements of separation point. In addition, the separation point at Re=300 for non-shear flow is 106.6 in the present simulation, which agrees closely with the corresponding angle of 106.5 obtained by Persillon and Braza (1998).

The flow field around the circular cylinder changes with the movements of stagnation point and separation points. Fig.6 compares the mean velocity profiles around a circular cylinder at several streamwise locations between non-shear or shear-flow conditions. The condition of Re=1000 and β=0.2 is shown as an example of shear flows. In the uniform flow condition, the flow accelerated symmetrically on both sides of the circular cylinder. In the shear flow condition, it can be observed that the flow on the low-velocity side accelerates greatly compared to that on the high-velocity side at all streamline locations. The velocity difference that the cylinder experienced is not as strong as in the oncoming flow. In other words, the asymmetry in the oncoming velocity profile is 'self-adjusted' to some extent by the cylinder itself. In our experimental study (Cao et. al., 2007), it was noticed that the

vortex shedding frequencies were the same on the two sides of the cylinder at location x/D=1.0. The acceleration was also noticed on the low-velocity side in the wake, but it was impossible to measure closely to the model to investigate the velocity field in the boundary layer near the separation point in the experiment. How the velocity difference between the high- and low-velocity sides varies with the shear parameter at the location of x/D=0 (center of the cylinder) is of interest to us. The location of maximum velocity in the velocity profile, like points H and L in Fig.6, corresponds generally to the location of the separated layer. Thus, the variations between the velocity differences at these two points, $\Delta U / U_c$ =(UH -UL)/UC , with shear parameter and Reynolds number have important meanings in understanding the flow mechanism. Fig.7 shows the variation of with shear parameter at x/D=0 by solid lines. Meanwhile, the velocity difference in the oncoming flow between the top and bottom of the cylinder is shown by a broken line for comparison. The magnitude of the shear parameter equals the velocity difference, i.e., β =0.2 means $\Delta U / U_c$ =(U_A-U_B)/U_C =0.2 (refer to Fig.1) in the oncoming flow. Fig.7 shows that the velocity difference experienced by the cylinder increases almost linearly with shear parameter for all Reynolds numbers, and is about 55% of that in the oncoming flow, except for Re=60. However, the velocity difference does not disappear. The strength and depth of the boundary layer, and then the vorticity generated in the separated shear layers, still differ on the two sides. For a given shear parameter, the velocity difference decreases with Reynolds number at low Reynolds numbers, and remains almost unchanged when the Reynolds number is greater than Re=500. It seems appropriate to assume that the velocity difference and then the unbalanced separated shear layer still exist at much higher Reynolds numbers.

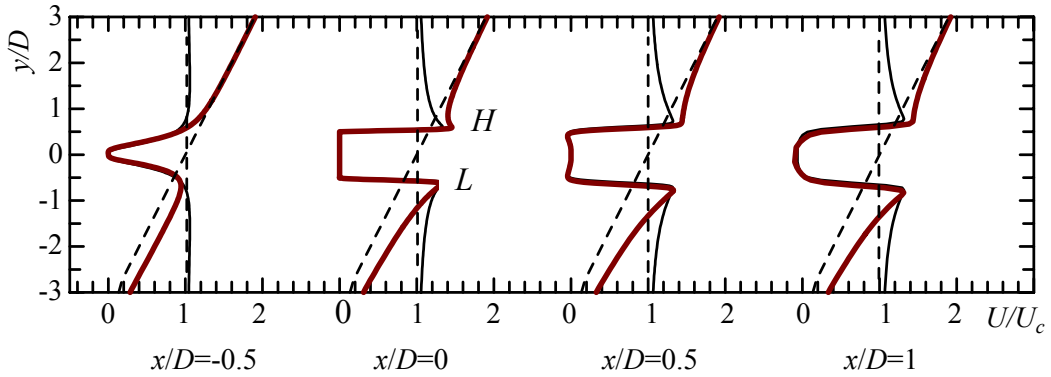

Fig.6 Mean velocity field around the cylinder (Re=1000, β = 0.2)
(- - -: Oncoming flow; ——: wake in non-shear flow; ▬: wake in shear flow)

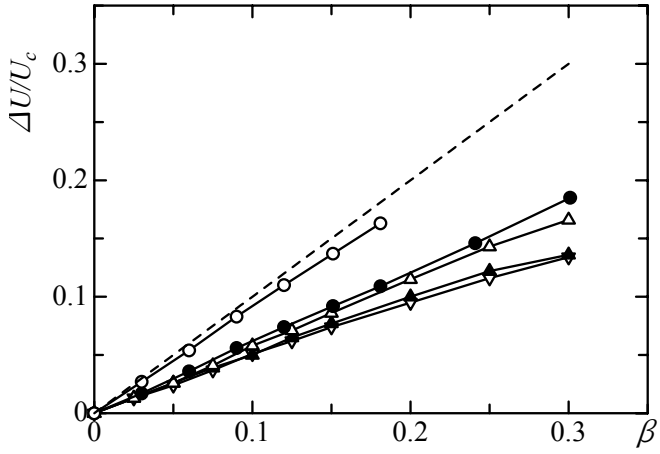

Fig.7 Variation of mean velocity difference with shear parameter at x/D=0
(○: Re=60; ●: Re=150; △: Re=200; ▲: Re=500; ▽: Re=1000;- - - : in oncoming flow)

3.2 Aerodynamic forces

Fig.8a compares the pressure distributions around a cylinder in non-shear and shear flows at Re=1000. θ=0 is the geometrical stagnation point on the forebody. The pressure coefficient C_p is defined as $C_p = (P - P_\infty)/(0.5\rho U_c^2)$, where P is the local mean pressure on the cylinder surface, is the pressure upstream of the cylinder, and ρ is the density of the fluid. The variations of stagnation point and separation points have been summarized above. Fig.8a shows that the pressure distribution around a circular cylinder is asymmetric in the shear flows. Movement of stagnation point to the high-velocity side is observed. The pressure coefficient is larger on the high-velocity side from the stagnation point to the point where the pressure is minimum (hereafter referred to as zone A, as shown in Fig.8b), while it is larger on the low-velocity side from the minimum pressure point to the separation point (hereafter referred to as zone B). The difference between the pressure coefficients on the high- and low-velocity sides increases with increasing shear parameter. There is no significant difference between the pressure coefficients on the two sides of the cylinder in the afterbody (hereafter referred to as zone C) because it is determined by the interaction of the two separated shear layers. Base pressure recovers slightly in shear flow, which is also observed in the experiment (Cao et al., 2007). Fig.8a shows that the separation point in the shear flow moves downstream on the high-velocity side, and moves upstream on the low-velocity side, and the movements of separation point are more significant with increase in shear parameter. The pressure distribution in zone A is mainly caused by the movement of stagnation point while that in zone B is mainly caused by the movement of separation points 8, which is a direct result of the difference between the velocities on the two sides of the cylinder. This means that the pressure distribution around the circular cylinder received the combined effects of movement of stagnation point and velocity shear. The variations of pressure distribution at other Reynolds numbers are not shown here because they are very similar to that at Re=1000, and the most important characteristics, the variation of separation point and separation points, have been presented above.

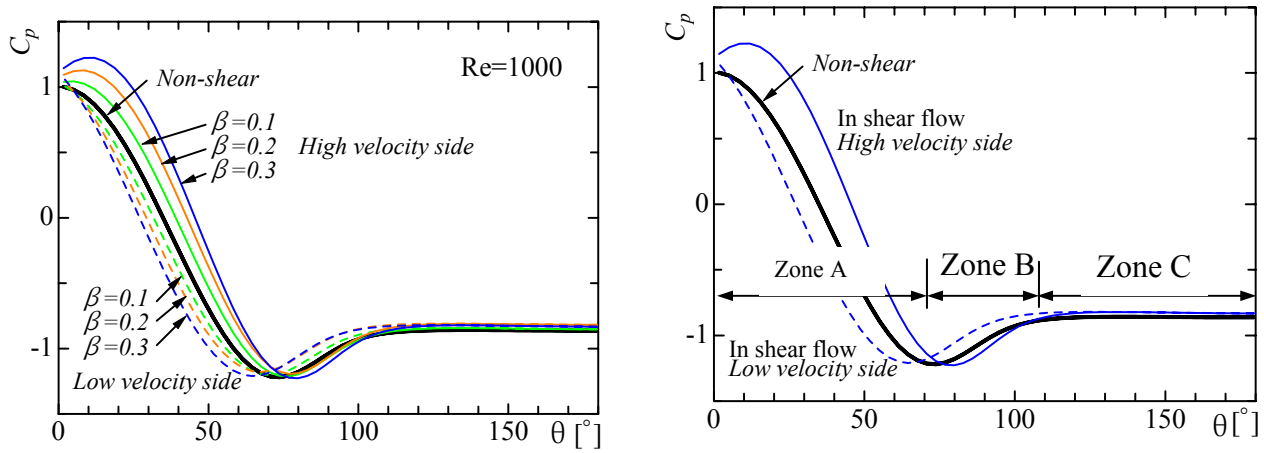

(a) Variation of pressure distribution (b) Zoning of pressure distribution

Fig.8 Variation of pressure distribution with shear parameter and its zoning

The drag and lift forces are determined from the sum of the friction force and pressure force around the cylinder. However, pressure force contributes more in this Reynolds number range. Consider the pressure distribution around a cylinder in a shear flow like that in Fig.8b. Compared to the pressure distribution in non-shear flow, in zone A, the increased pressure on the high-velocity side and the decreased pressure on the low-velocity side cancel each other out to some extent when considering their contributions to drag force. The increased pressure on the low-velocity side and the decreased pressure on the high-velocity side in zone B also cancel each other out. Recovery of the base pressure in the shear flow in zone C leads to a reduction in drag coefficient. Whether the drag is increased or decreased depends on the sum of these contributions. This characteristic determines that

the variation of drag coefficient with shear parameter is not great whether it increases or decreases in the shear flows. Fig.9 shows the variation of drag coefficient with shear parameter at all investigated Reynolds numbers, with the comparison of experimental results by Sumner and Akosile (2003) and Cao et al. (2007) and the numerical result of Lei et al. (2000). Reynolds number dependence of drag coefficient can be observed in the present simulation results. Fig.9 shows that the increase or decrease in drag coefficient with shear parameter is so small that it seems appropriate to consider it as unchanged with shear parameter. The numerical results of Lei et al. (2000) at Re=200 and Re=600 in Fig.9 present a tendency of decrease in drag coefficient with increase in shear parameter. However, their simulation is two-dimensional and even the drag in the non-shear condition showed significant differences from the present 3D simulation results. However, the present simulation shows obvious differences from our experimental results (Cao et al., 2007). The difference between the turbulence intensities of the simulation and experiment is considered as the reason for this. The turbulence intensity increased with shear parameter from 2% to 6% in the experiment, which greatly influenced the experimental results. Adachi and Kato (1975) also remarked that their observation of the drag force change in shear flow is possibly caused by the increased turbulence intensity. In respect of the

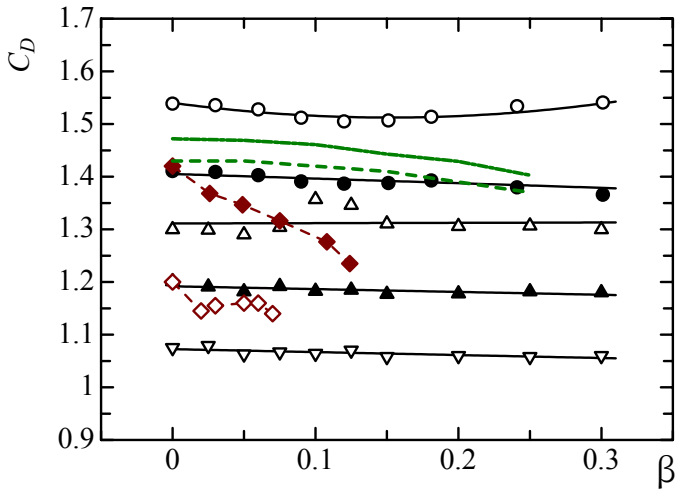

Fig.9 Variation of drag coefficient with shear parameter at different Reynolds numbers
(○: Re=60; ●: Re=150; △: Re=200; ▲Re=500; ▽: Re=1000, ◇Sumner and Akosile (2003);
◆: Cao et al. (2007); – –: Re=200, Lei et al. 2000; ·····: Re=600, Lei et al., 2000)

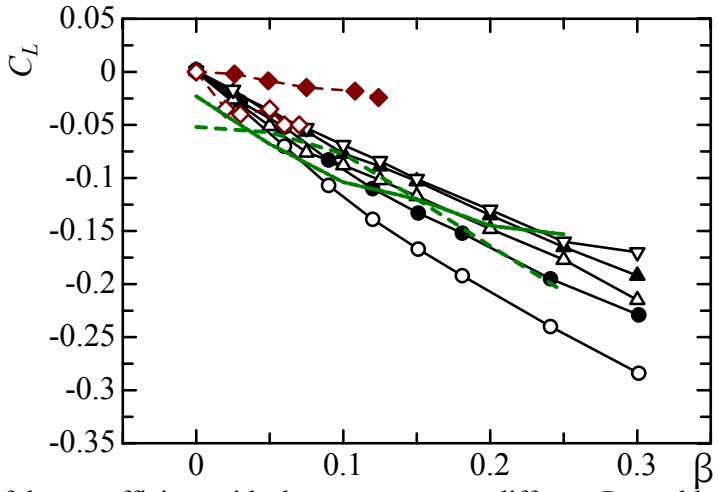

Fig.10 Variation of drag coefficient with shear parameter at different Reynolds numbers
(○: Re=60; ●: Re=150; △: Re=200; ▲: Re=500; ▽: Re=1000; ◇: Sumner and Akosile (2003);
◆: Cao et al. (2007); – –: Re=200, Lei et al., 2000;····· : Re=600, Lei et al., 2000)

pure shear effects, the present study shows that it influences the drag coefficients very slightly. In addition, like to the results of Strouhal number, there is discontinuity in the change of drag coefficient, as shown in Fig.9, with shear parameter because of the mode change. The magnitude of drag coefficient depends greatly on Reynolds number, but the Reynolds number effect on the variation of drag coefficient with shear parameter is small.

However, the mean lift force, which does not occur in uniform flow, exists due to the asymmetry of the pressure distribution. Although the pressure is larger on the low-velocity side in zone B, which creates a lift force from the low-velocity side to the high-velocity side, it is larger on the high-velocity side in zone A, which creates a lift force from the high-velocity side to the low-velocity side. Fig.10 shows that the resultant lift force acts from the high-velocity side to the low-velocity side, which means that contribution from the movement of stagnation point is larger. Increase in lift force with direction from the high- to the low-velocity sides was also reported by Sumner and Akosile (2003), Cao et al. (2007) in an experimental study and Lei et al. (2000) in a numerical study. Tamura et al. (1980) investigated numerically the variation of drag and lift forces with shear parameter at Re=40 and 80. They reported that the lift force increases with shear parameter, as in the present study, but the lift force was shown to act from the low-velocity side to the high-velocity side. They explained this as the result of smaller minimum pressure at θ =90 o on the high-velocity side, which creates a lift force toward the high-velocity side. The contribution of the movement of stagnation point was not mentioned in their study. Reynolds number greatly influences the variation of lift coefficient with shear effect.

The above results confirmed and added new information to the mechanism of flow around a circular cylinder proposed by Cao et al. (2007). In the fore-body of a cylinder (zone A), the stagnation point moves to the high-velocity side, so the flow on the low-velocity side is more accelerated than on the high-velocity side. This leads to low pressure on the low-velocity side. Movement of stagnation point is mainly influenced by the shear parameter. Reynolds number has little influence in determining the movement of stagnation point. After that, in zone B, the velocity difference between the two sides functions dominantly and results in larger pressure on the low-velocity side. Reynolds number greatly influences the variation of separation point with shear parameter. The drag and lift forces are determined by the individual distribution of two factors: movement of stagnation and velocity shear. However, considering their performances around the cylinders, it can be concluded that the drag force was little influenced by the velocity of the oncoming shear flow while the lift force was greatly influenced by it, and the lift force acts from the high-velocity side to the low-velocity side.

4. CONCLUSIONS

Three-dimensional Direct Numerical Simulation (DNS) and Large Eddy Simulation (LES) are performed to investigate the shear effects on the flow around a circular cylinder at Reynolds numbers of Re=60-1000. Variations of Strouhal number, drag and lift coefficients and unsteady wake structures with shear parameter, and their dependences on Reynolds number are studied.

The Strouhal number is almost unchanged in the shear parameter range of 0-0.30 at Re=60-1000. Three-dimensionality of mode A wake instability is suppressed to two-dimensional parallel vortex shedding at Re=200. The onset of mode A three-dimensionality is delayed by velocity shear. Karmax vortex shedding was not completely suppressed in the investigated range of Reynolds numbers and shear parameters. However, the vortices on the low-velocity side disappear in the far wake in the strong shear parameter condition. Large acceleration occurs on the low-velocity side, which self-adjusts the asymmetry in the oncoming flow in the near wake of the cylinder.

The stagnation point moves to the high-velocity side in shear flows. The movement of the angle of the stagnation point increases with shear parameter. The Reynolds number has little influence in

determining the movement of the stagnation point. The separation point moves downstream on the high-velocity side and upstream on the low-velocity side. The movement of the angle of the separation point increases with shear parameter. Reynolds number greatly influences the magnitude of movements of separation points.

Movement of stagnation point and velocity shear influences the pressure distribution around the cylinder simultaneously, but with opposite contribution. In the range of Re=60-1000 and 0< <0.3, drag force is almost unchanged with increasing shear parameter. Lift force occurs in the shear flow due to the asymmetry of pressure distribution around the cylinder, and acts from the high-velocity side to the low-velocity side. Movement of the stagnation points contributes more to the lift force than the velocity shear.

Acknowledgements

This study was funded by the Ministry of Education, Culture, Sports, Science and Technology, Japan, through the Global COE Program, 2008-2012.

REFERENCES

Adachi T., Kato E., 1975. Study on the flow about a circular cylinder in shear flow. Transactions of the Japan Society for Aeronautical and Space 256, 45-53.

Cao S., Ozono S., Hirano K., Tamura Y., 2007. Vortex shedding and aerodynamic forces on a circular cylinder in linear shear flow at subcritical Reynolds number. Journal of Fluids and Structures 23, 703-714.

Cao S., Tamura Y. (2008): Flow around a circular cylinder in linear shear flows at subcritical Reynolds number, Journal of wind engineering and industrial aerodynamics, 96, 1961-1973.

Cao S., Tamura Y. (2009): Suppression of three dimensionality of vortex shedding by strong velocity shear, Journal of Fluids and Structures. In submission.

Germano M., Piomelli U., Moin P., Cabot W.H., 1991. A dynamic subgrid-scale viscosity model, Physics of Fluids, A Vol.3 No.7, pp.1760-1765.

Hayashi T., Yoshino F., 1990. On the evaluation of the aerodynamic forces acting on a circular cylinder in a uniform shear flow. Transactions of the Japan Society for Mechanical Engineering 56, No.552, 31-36.

Kim J. and Moin P. (1985) Application of a fractional-step method to incompressible Navier-Stokes equations, Journal of computational physics 59, 308-323.

Kiya M., Tamura H., Arie M., 1980. Vortex shedding from a circular cylinder in moderate-Reynolds- number shear flow. Journal of Fluid Mechanics 141, 721-735.

Kwon T.S., Sung H.J., Hyun J. M., 1992. Experimental investigation of uniform shear flow past a circular cylinder. ASME Journal of Fluids Engineering 114, 457-460.

Kravchenko A.G and Moin P., 2000. Numerical studies of flow over a circular cylinder at Re=3900, Physics of fluids 12, No.2, 403-417.

Lei, C., Cheng, L., Kavanagh, K., 2000. A finite difference solution of the shear flow over a circular cylinder, Ocean Engineering 27, 271-290.

Lilly D.K., 1992. A proposed modification of the Germano subgrid-scale closure model, Physics of Fluids, A. Vol.4 No.4, pp.633-635.

Persillon H, Braza M. Physical analysis of the transition to turbulence in the wake of a circular cylinder by three-dimensional Navier-Stokes simulation. Journal of Fluids Mechanics 1998; 365: 23-88.

Sumner D., Akosile O.O, 2003. On uniform planar shear flow around a circular cylinder at subcritical Reynolds number, Journal of Fluids and Structures 13, 309-338.

Zang Y, Street R.L. and Koseff J.R., 1994. A non-staggered grid, fractional step method for time-dependent incompressible Navier-Stokes equations in curvilinear coordinates, Journal of Computational Physics 114, 18-33.

Tamura H., Kiya M., Arie M., 1980. Numerical study of viscous shear flow past a circular cylinder. Transactions of the Japan Society for Mechanical Engineering 46, No.404, 555-564.

Tamura T. and Kitagishi T., 2001. Application of the interpolation method in generalized coordinate system to wake flows around a circular cylinder, J. Struct. Constr. Eng., AIJ, 545, 27-34.

Tamura T., 2008. Towards practical use of LES in wind engineering, Journal of Wind Engineering and Industrial Aerodynamics, 96 (10-11), 1451-1471.

Williamson C.H.K., 1996. Vortex dynamics in the cylinder wake, Annu. Rev. Fluid Mech. 28, 477.

Zhang H.Q, Fey U., Noack B.R., 1995. On the transition of the cylinder wake, Phys. Fluids 7(4) 779-794.